



## Estimating long-term PM<sub>2.5</sub> concentrations in China using satellite-based aerosol optical depth and a chemical transport model



Guannan Geng<sup>a,b,c</sup>, Qiang Zhang<sup>a,\*</sup>, Randall V. Martin<sup>b,d</sup>, Aaron van Donkelaar<sup>b</sup>, Hong Huo<sup>e</sup>, Huizheng Che<sup>f</sup>, Jintai Lin<sup>g</sup>, Kebin He<sup>c</sup>

<sup>a</sup> Ministry of Education Key Laboratory for Earth System Modeling, Center for Earth System Science, Tsinghua University, Beijing 100084, China

<sup>b</sup> Department of Physics and Atmospheric Science, Dalhousie University, Halifax, NS B3H 4R2, Canada

<sup>c</sup> State Key Joint Laboratory of Environment Simulation and Pollution Control, School of Environment, Tsinghua University, Beijing 100084, China

<sup>d</sup> Harvard-Smithsonian Center for Astrophysics, Cambridge, MA 02138, USA

<sup>e</sup> Institute of Energy, Environment and Economy, Tsinghua University, Beijing 100084, China

<sup>f</sup> Key Laboratory of Atmospheric Chemistry (LAC), Institute of Atmospheric Composition, Chinese Academy of Meteorological Science, Beijing 100081, China

<sup>g</sup> Laboratory for Climate and Ocean-Atmosphere Studies, Department of Atmospheric and Oceanic Sciences, School of Physics, Peking University, Beijing 100871, China

### ARTICLE INFO

#### Article history:

Received 17 September 2014

Received in revised form 16 April 2015

Accepted 20 May 2015

Available online 9 June 2015

#### Keywords:

Particulate matter

Aerosol optical depth

Satellite remote sensing

### ABSTRACT

Epidemiological and health impact studies of fine particulate matter (PM<sub>2.5</sub>) have been limited in China because of the lack of spatially and temporally continuous PM<sub>2.5</sub> monitoring data. Satellite remote sensing of aerosol optical depth (AOD) is widely used in estimating ground-level PM<sub>2.5</sub> concentrations. We improved the method for estimating long-term surface PM<sub>2.5</sub> concentrations using satellite remote sensing and a chemical transport model, and derived PM<sub>2.5</sub> concentrations over China for 2006–2012. We generated a map of surface PM<sub>2.5</sub> concentrations at 0.1° × 0.1° over China using the nested-grid GEOS-Chem model, most recent bottom-up emission inventory, and satellite observations from the MODIS and MISR instruments. Aerosol vertical profiles from the space-based CALIOP lidar were used to adjust the climatological drivers of the bias in the simulated results, and corrections were made for incomplete sampling. We found significant spatial agreement between the satellite-derived PM<sub>2.5</sub> concentrations and the ground-level PM<sub>2.5</sub> measurements collected from literatures ( $r = 0.74$ , slope = 0.77, intercept = 11.21 μg/m<sup>3</sup>). The population-weighted mean of PM<sub>2.5</sub> concentrations in China is 71 μg/m<sup>3</sup> and more than one billion people live in locations where PM<sub>2.5</sub> concentrations exceed the World Health Organization Air Quality Interim Target-1 of 35 μg/m<sup>3</sup>. The results from our work are substantially higher than previous work, especially in heavily polluted regions. The overall population-weighted mean uncertainty over China is 17.2 μg/m<sup>3</sup>, as estimated using ground-level AOD measurements and vertical profiles observed from CALIOP.

© 2015 Elsevier Inc. All rights reserved.

### 1. Introduction

Chronic exposure to fine particulate matter with aerodynamic diameters of less than 2.5 μm (PM<sub>2.5</sub>) is associated with increased cardiovascular and respiratory morbidity, and all-cause mortality (Dockery et al., 1993; McDonnell, Nishino-Ishikawa, Petersen, Chen, & Abbey, 2000; Pope et al., 2002). Following the rapid economic development and urbanization in China, levels of PM<sub>2.5</sub> have become the highest in the world (van Donkelaar et al., 2010). However, epidemiological studies have been limited in China because of the lack of spatially and temporally continuous data regarding PM<sub>2.5</sub> exposure. Prior to 2013, there was no official nationwide PM<sub>2.5</sub> dataset and only research groups had implemented a number of monitoring sites (Yang et al., 2011). Since

January 2013, a national network for PM<sub>2.5</sub> monitoring has been established, which encompasses all the provincial capital cities and some other major cities. Unfortunately, even this network has limited geographical coverage and most of the monitoring sites are located in urban areas. Furthermore, point measurements alone are unable to provide information on regional variable concentrations and therefore, additional observations are needed to improve our understanding on the spatial patterns of ambient PM<sub>2.5</sub> concentrations over China.

Advances in satellite remote sensing have provided valuable insights into surface air quality (Hoff & Christopher, 2009; Martin, 2008). Satellite-based estimates of PM<sub>2.5</sub> concentrations are useful supplements to ground-based PM<sub>2.5</sub> measurements because of their broad spatiotemporal coverage. The Moderate Resolution Imaging Spectroradiometer (MODIS) and the Multi-angle Imaging SpectroRadiometer (MISR) onboard the Terra satellite, launched by the National Aeronautics and Space Administration (NASA), offer global observations of aerosol optical depth (AOD), which is defined as the integrated extinction by aerosol

\* Corresponding author.

E-mail address: [qiangzhang@tsinghua.edu.cn](mailto:qiangzhang@tsinghua.edu.cn) (Q. Zhang).

over a vertical column of unit cross section (Diner et al., 1998; Kahn, Banerjee, McDonald, & Diner, 1998; Levy, Remer, Mattoo, Vermote, & Kaufman, 2007; Remer et al., 2005). AOD is sensitive to fine particles and it has been proven well correlated to PM<sub>2.5</sub> concentrations (Chu et al., 2003; Engel-Cox, Hoff, & Haymet, 2004). However, a quantitative PM<sub>2.5</sub>/AOD relationship is needed in order to assess PM<sub>2.5</sub> concentrations quantitatively using AOD.

Many studies have investigated the relationship between column AOD and surface PM<sub>2.5</sub> concentrations using statistical models (Che, Yang, Zhang, Zhu, Ma, Zhou, et al., 2009; Hu et al., 2013; Kloog, Nordio, Coull, & Schwartz, 2012; Lee, Liu, Coull, Schwartz, & Koutrakis, 2011; Ma, Hu, Huang, Bi, & Liu, 2014). Early studies using simple linear regression models obtained reasonable results (Wang & Christopher, 2003); however, this relationship could not be extended to other regions or times because of the effects of variations in emissions and meteorological conditions (Zhang, Hoff & Engel-Cox, 2009). Recent studies have involved more advanced regression models and meteorological parameters, to improve the representation of the relationship between AOD and PM<sub>2.5</sub>, resulting in significantly enhanced estimates of PM<sub>2.5</sub> concentrations (Beckerman et al., 2013; Hu et al., 2014). Ma et al. (2014) recently took advantage of the newly established Chinese national monitoring network and estimated the PM<sub>2.5</sub> concentrations over China in 2013 from MODIS and MISR AOD using geographically weighted regression (GWR) model. However, statistical models rely largely on ground measurements of PM<sub>2.5</sub> data, which were not available before 2013 in China.

Another common method for simulating the AOD–PM<sub>2.5</sub> relationship is using the chemical transport model to provide the spatiotemporal variability of the PM<sub>2.5</sub>/AOD ratio. Liu et al. (2004) proposed the method first and estimated PM<sub>2.5</sub> concentrations over the United States from MISR observations. Later, van Donkelaar et al. (2010) extended the method to the global scale using combined MODIS and MISR data and obtained the first global surface PM<sub>2.5</sub> concentration map for the period of 2001–2006. This method has also been applied to a case study of biomass burning, demonstrating this approach can be applicable even during extreme events, which are quite frequent for PM<sub>2.5</sub> levels in China (van Donkelaar et al., 2011). The most important factor affecting the relationship between AOD and PM<sub>2.5</sub> is often the relative vertical profile (van Donkelaar, Martin, & Park, 2006), which can be evaluated and adjusted, as necessary, by lidar retrievals from the Cloud-Aerosol Lidar with Orthogonal Polarization (CALIOP) instrument (van Donkelaar et al., 2013).

In this study, we update the estimation of surface PM<sub>2.5</sub> concentrations over China to 2006–2012 using a nested-grid chemical transport model and recent bottom-up emission inventory, with improvements of other correction factors. We use the nested-grid GEOS-Chem model to calculate the PM<sub>2.5</sub>/AOD conversion factors and then apply these factors to the combined MODIS and MISR AOD data. The satellite-based surface PM<sub>2.5</sub> concentrations are developed at a resolution of 0.1° × 0.1° over China with the error estimates. Finally, the results are validated against ground-based measurements and applied to human exposure calculations.

## 2. Materials and methods

### 2.1. Ground-based PM<sub>2.5</sub> measurements

Since the national PM<sub>2.5</sub> air quality monitoring networks in China were not established until 2013, measurements for 2006–2012 were collected from literatures. The sources of the data, site locations, sampling period, and other information are all listed in Table S1. In addition, daily PM<sub>2.5</sub> measurements from 2013 were collected from the official website of the China Environmental Monitoring Center (CEMC) (<http://113.108.142.147:20035/emcpublish/>) as a supplemental validation dataset of our work, which covers 74 cities in China. According to the Chinese National Ambient Air Quality Standard (CNAAQs,

GB3095–2012, <http://kjs.mep.gov.cn/hjbhbz/bzwb/dqhjbh/dqhjzlbz/201203/W020120410330232398521.pdf>) released in 2012, the ground-based PM<sub>2.5</sub> data are measured by the tapered element oscillating microbalance technology (TEOM) or the beta-attenuation method.

### 2.2. Ground-based AOD measurements

AOD measurements from two ground networks, Aerosol Robotic Network (AERONET, Holben et al., 1998) and China Aerosol Remote Sensing Network (CARSNET, Che, Zhang, Chen, Damiri, Goloub, Li, et al., 2009) were collected to filter the satellite AOD with large bias. The spatial distributions of the two ground networks over China are shown in Fig. S1. AERONET is a world-wide aerosol monitoring network and has been widely used for evaluation of satellite remote sensing or model simulations (Kahn, Garay, Nelson, Yau, Bull, Gaitley, et al., 2007; Lin, van Donkelaar, Xin, Che, & Wang, 2014; van Donkelaar et al., 2010). However, AERONET only has a few long-term monitoring sites over China. CARSNET, which was established by the China Meteorological Administration in 2002, is a Chinese aerosol monitoring network for aerosol optical property study using the same CE-318 sunphotometers as AERONET. AOD data at 550 nm are derived using values at 440 nm wavelength and the associated Ångström exponent in both AERONET and CARSNET data.

### 2.3. Satellite observations

The MODIS instrument onboard the Terra satellite measures a wide range of spatial and spectral information, providing global coverage in 1–2 days at a resolution of 10 × 10 km (Levy et al., 2007). The MISR instrument, which is also onboard the Terra satellite, uses same-scene, multi-angle, multi-spectral observations, providing global coverage in 2–9 days at a resolution of 18 × 18 km (Kahn, Li, Moroney, Diner, Martonchik & Fishbein, 2007). The MODIS collection 5.1 level 2 products (MOD04) and the MISR version 22 level 2 products at 550 nm for 2006–2013 are used in this study. Both AOD retrievals are obtained under cloud-free conditions.

The MODIS BRDF/Albedo product (MCD43B3) estimates 16-day average land surface albedo using a kernel-driven semi-empirical BRDF model (Schaaf et al., 2002). It provides both the directional hemispherical reflectance (black-sky albedo) and the bi-hemispherical reflectance under isotropic illumination (white-sky albedo), which are two extremes of the true albedo. The 7-year black-sky albedo data at three wavelengths, 0.47 μm, 0.66 μm and 2.1 μm, are used in this study to identify different surface types.

The CALIOP instrument onboard the Cloud-Aerosol Lidar and Infrared Pathfinder Satellite Observation (CALIPSO) satellite has been acquiring global profiles of aerosol and cloud since 2006 (Winker, Hunt, & McGill, 2007). CALIOP emits simultaneous, co-aligned pulses at 1064 nm and 532 nm from its laser and observes the backscattered radiation by a 1-meter diameter telescope. Extinction profiles at a resolution of 30 m vertical and 333 m horizontal are retrieved and widely used for validation of modeled vertical profile and their impact on satellite-derived PM<sub>2.5</sub> (Toth et al., 2014; van Donkelaar et al., 2013).

### 2.4. Combining MODIS and MISR AOD

Satellite AOD retrievals have regional biases compared to ground measurements and surface reflectance is a major source of uncertainties. To reduce the bias and combine the two products reasonably, van Donkelaar et al. (2010) has developed a method to distinguish surface types using black-sky albedo and identify regional errors in AOD retrievals by extending biases calculated against ground measurements within a certain surface type.

Following the method described by van Donkelaar et al. (2010), we used two ratios of the 7-year monthly mean black-sky albedo (0.47 μm / 0.66 μm and 0.66 μm / 2.1 μm) from the MODIS BRDF/Albedo products

to divide China region into nine categories, as defined by the combinations of each ratio being <0.4, 0.4–0.6, and >0.6. Four surface types dominate over China. We used the ground AOD measurements during 2006–2012 to calculate the monthly mean bias of satellite AOD and interpolated in each defined surface type category using inverse distance weighting method for both MODIS and MISR. Daily satellite AOD data from either MODIS or MISR with a corresponding monthly bias larger than  $\pm 20\%$  or  $\pm 0.1$  were excluded and the bias-filtered MODIS and MISR data were averaged to offer estimates of final long-term retrieval. All the data were regridded to  $0.1^\circ \times 0.1^\circ$  resolution. The combination of MODIS and MISR retrievals proved to offer estimates of AOD that were more reliable and with greater spatial coverage than estimates from either instrument alone (van Donkelaar et al., 2010).

## 2.5. Estimating $PM_{2.5}$ from AOD

Chemical transport models are used to provide the spatially and temporally resolved conversion factors to calculate the satellite-derived surface  $PM_{2.5}$  concentrations, and vertical correction factors from CALIOP instrument are used to correct the model simulations, as defined in Eq. (1) (Liu et al., 2004; van Donkelaar et al., 2013):

$$[PM_{2.5,satellite}]_{i,j} = [AOD_{satellite}]_{i,j} \cdot \frac{[PM_{2.5,model}]_{i,j}}{\sum_{v=1}^{47} [AOD_{model}]_{i,j,v} \cdot \alpha_{i,k,v}} \quad (1)$$

where  $[PM_{2.5,satellite}]_{i,j}$  and  $[PM_{2.5,model}]_{i,j}$  represent the  $PM_{2.5}$  concentrations derived from the satellite or the model simulation at a grid  $i$  on a day  $j$ , respectively;  $[AOD_{satellite}]_{i,j}$  is the satellite AOD value at a grid  $i$  on a day  $j$ ;  $[AOD_{model}]_{i,j,v}$  is the modeled AOD at a grid  $i$  on a day  $j$  of a model layer  $v$  (47 layers in total);  $\alpha_{i,k,v}$  is the vertical correction factor obtained from the CALIOP observations at a grid  $i$  on a month  $k$  that corresponds to the day  $j$  of a model layer  $v$ .

In this study, the nested-grid GEOS-Chem model v9-01-02 over China with resolution of  $0.5^\circ \times 0.667^\circ$  (<http://geos-chem.org>; also see Supporting information) was utilized to simulate the temporal and spatial distribution of aerosol and gaseous concentrations for 2006–2012. This model was driven by assimilated meteorological data from the Goddard Earth Observing System (GEOS-5) at the NASA Global Modeling Assimilation Office (GMAO), and by the year-by-year emissions over China taken from the Multi-resolution Emission Inventory for China (MEIC; see Supporting information) developed by Tsinghua University. Lateral boundary conditions were provided by a global GEOS-Chem simulation with a resolution of  $2^\circ \times 2.5^\circ$ . The 24-h  $PM_{2.5}$  concentration in the bottom layer of the model was taken to represent the ground-level concentration. The simulated AOD at a wavelength of 550 nm between 10:00 and 12:00 local solar time were averaged, corresponding to the Terra satellite overpass time. Daily conversion factor maps were linearly interpolated from a model with resolution of  $0.5^\circ \times 0.667^\circ$  to  $0.1^\circ \times 0.1^\circ$  for application to the satellite AOD.

Aerosol vertical profiles are the most important factor affecting the ratios between  $PM_{2.5}$  and AOD (van Donkelaar et al., 2006). CALIOP observations provide valuable information to adjust potential sources of long-term bias in the model simulation, such as the modeled representation of vertical mixing or emissions. Following van Donkelaar et al. (2013), we used retrievals from the CALIOP instrument to evaluate and correct the simulated aerosol vertical profiles. Aerosol optical properties in CALIOP profiles are first adjusted to be consistent with that in model simulations. Aerosol profiles in the model simulations are then scaled according to the ratios of the simulated to retrieved relative vertical profiles, normalized to the surface model layer over a three-month running average. During this process, model simulations below the CALIOP detection limit are removed to allow for direct comparison between model and satellite (Ford & Heald, 2012). CALIOP retrievals with cloud and aerosol detection score less than 20 are also

rejected. The AOD columns calculated from the corrected profiles are used to infer satellite-based  $PM_{2.5}$ , as shown in Eq. (1). Although the spatial and temporal resolution of the CALIOP observation is insufficient to do the day-to-day correction, the climatological drivers of the bias have been adjusted, which is crucial to the long-term  $PM_{2.5}$  estimates.

We also accounted for sampling bias in satellite-derived  $PM_{2.5}$  concentrations, which is especially large in China because AOD data are usually missing when  $PM_{2.5}$  concentrations are high (van Donkelaar et al., 2011). The sampling bias correction factor is defined in Eq. (2) and its application in Eq. (3):

$$\beta_{i,k} = \frac{\sum_{j=1}^{N_k} [PM_{2.5,model}]_{i,j}}{M_{i,k}} \cdot \frac{M_{i,k}}{N_k} \quad (2)$$

$$[CorrectedPM_{2.5}]_i = \frac{\sum_k [PM_{2.5,satellite}]_{i,k} \cdot \beta_{i,k} \cdot N_k}{\sum_k N_k} \quad (3)$$

where  $\beta_{i,k}$  is the sampling bias correction factor at a grid  $i$  in a month  $k$ ;  $N_k$  is the number of days in a month  $k$  and  $M_{i,k}$  is the number of days that the model sampled coincidentally with the satellite observations at a grid  $i$  for the month  $k$ ;  $[PM_{2.5,satellite}]_{i,k}$  is the monthly mean data of the original satellite-derived  $PM_{2.5}$  concentrations in a month  $k$ ;  $[CorrectedPM_{2.5}]_i$  is the final retrieved long-term  $PM_{2.5}$  concentration at the grid  $i$ . For a given model grid  $i$ , the sampling correction factor is calculated as the ratio of full-month mean modeled concentration to that of model sampled with satellite data. The scale factor is then used to correct the derived monthly mean  $PM_{2.5}$  concentrations before long-term averaging.

## 3. Results

### 3.1. Input factors for $PM_{2.5}$ estimate

Mean AOD values for 2006–2012 obtained from MODIS and MISR over China are presented in Fig. 1. Both the MODIS and MISR AOD show consistent spatial distributions with large enhancements over the North China Plain, Yangtze River Delta, and Sichuan Basin, which are all places with high anthropogenic emissions (Zhang, Streets, Carmichael, He, Huo, Kannari, et al., 2009). The MODIS retrievals are not valid in part of northwestern China because of the bright surface of the Taklimakan Desert; however, MISR can successfully retrieve AOD in this region. In background areas with AOD of less than 0.2–0.3, the MODIS and MISR AOD are quite similar, while in other places the MISR AOD is systematically lower than MODIS with the difference reaching 0.35 in eastern China. The MISR version 22 is known to underestimate AOD frequently over land when AOD exceeds about 0.6 because of the improper partitioning of the radiance, i.e., more top-of-atmosphere signal is assigned to the surface by the MISR heterogeneous-land component of the over-land algorithm (Chen, Kahn, Nelson, Yau, & Seinfeld, 2008; Kahn et al., 2010). AOD is also underestimated when the absorbing aerosol particles have smaller single-scattering albedo than those included in the retrieval algorithm climatology (Chen et al., 2008; Kahn et al., 2010). After the filtration and combination process of the two sets of satellite data, the biased AOD is removed and an almost full spatial coverage over China is obtained (Fig. 1c). The combined AOD map is dominated by MODIS in the east because of the underestimation by MISR over high-value regions, and dominated by MISR in the west because of MISR's ability to retrieve data over bright surfaces. We also select four polluted regions (Fig. 1c)

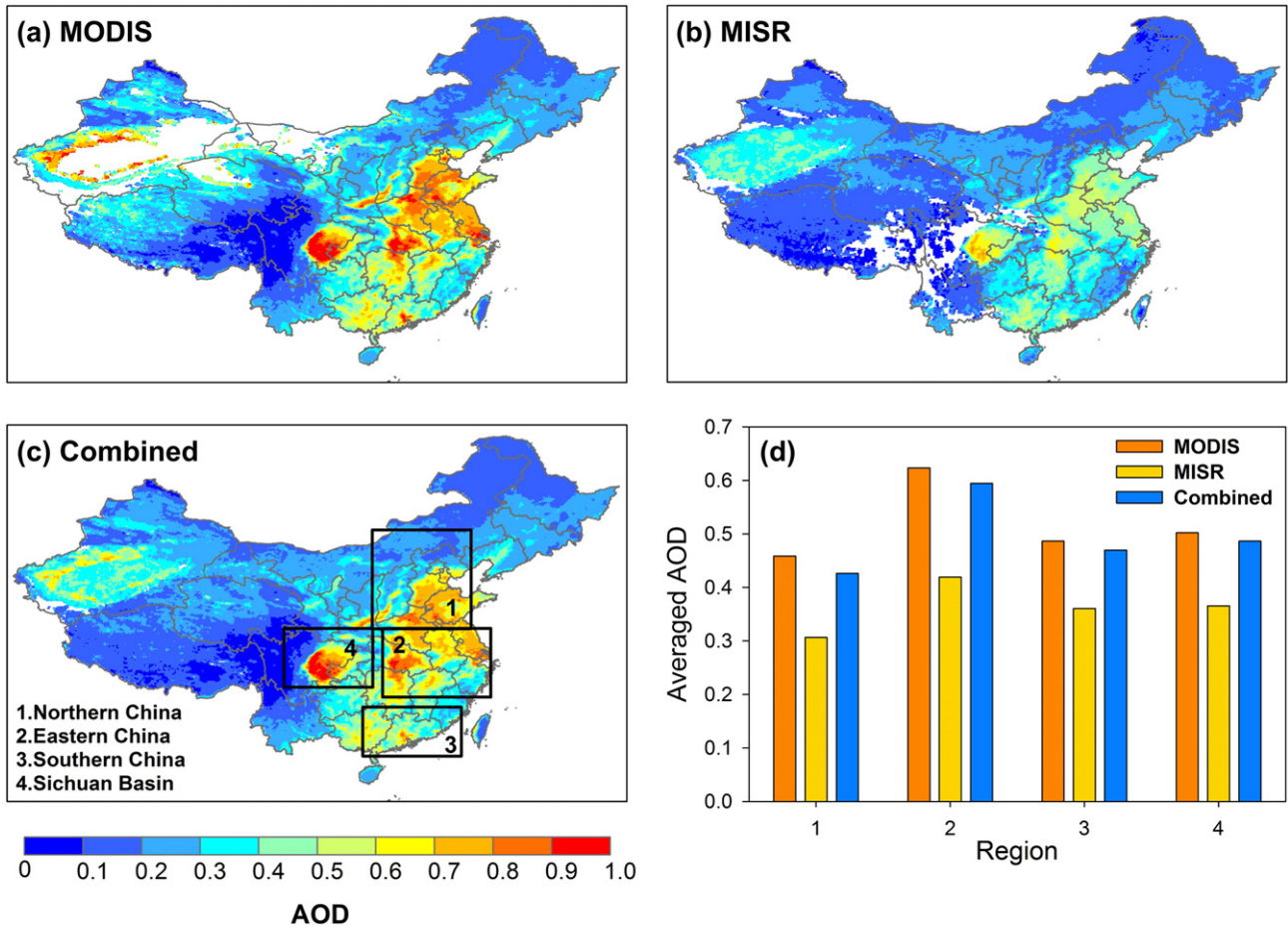


**Fig. 1.** Averaged AOD for 2006–2012 (a) from the MODIS Terra satellite instrument, (b) from the MISR satellite instrument, (c) from the combined product developed in this study, and (d) in four selected regions. White denotes less than 10 successful satellite observations. Boxed areas outline the regions used in this figure and Fig. 2, which are Northern China (110°E–120°E, 34°N–44°N), Eastern China (111°E–122°E, 27°N–34°N), Southern China (109°E–119°E, 21°N–26°N) and Sichuan Basin (101°E–110°E, 28°N–34°N).

and present the regional averaged AOD in Fig. 1d. Eastern China has the highest AOD value of the four regions, possibly due to its large anthropogenic emissions and relatively high humidity.

Fig. 2 shows the spatial distribution and regional average of the seven-year mean conversion factors used to derive  $PM_{2.5}$  concentrations from the AOD. The conversion factors are mainly affected by

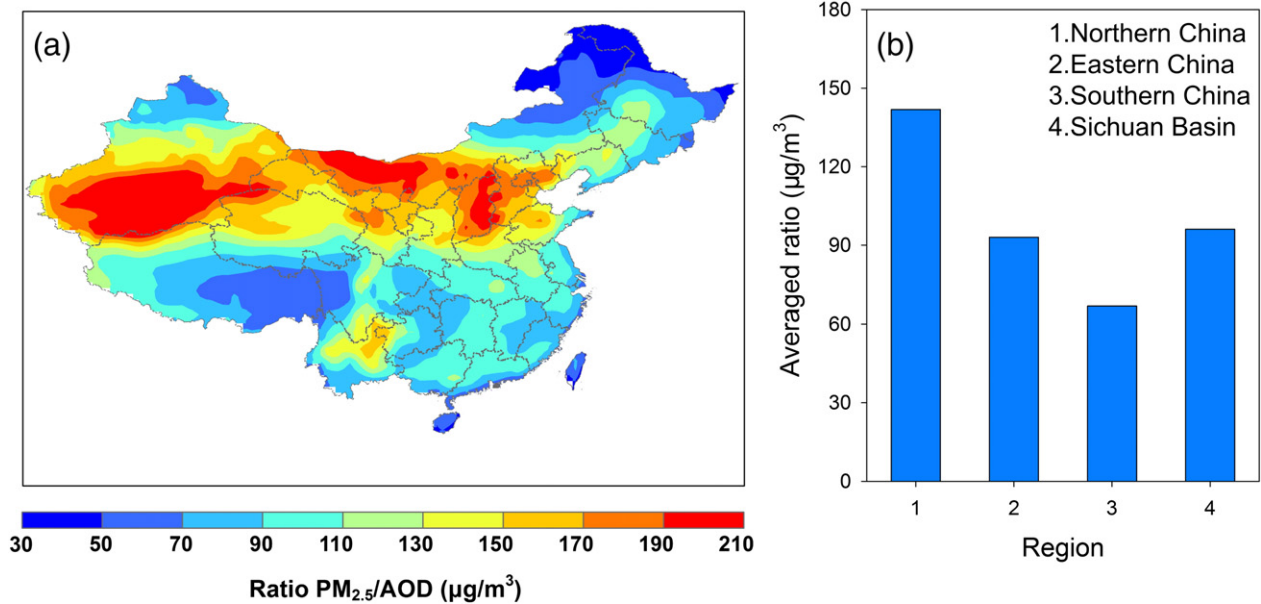


**Fig. 2.** (a) Spatial distribution and (b) regional mean of the averaged ratio of  $PM_{2.5}$  to AOD for 2006–2012.

aerosol type, meteorological conditions, and aerosol vertical structures. High values lie in regions with relatively large fractions of aerosols near the ground, as well as places with greater low-hygroscopic components (e.g., mineral dust) because of its low contribution of aerosol water to AOD. Large enhancements of conversion factors above  $170 \mu\text{g}/\text{m}^3$  are found over the northwest parts, which are consistent with the spatial distribution of dust storms in China (Sun, Zhang, & Liu, 2001). Values between  $90\text{--}150 \mu\text{g}/\text{m}^3$  are also found over most of northern and eastern China, which are related to industrial regions with surface aerosol sources.

### 3.2. Satellite-derived $\text{PM}_{2.5}$ concentrations for 2006–2012

The 7-year mean 24-h-average satellite-derived surface  $\text{PM}_{2.5}$  concentrations over China are presented in Fig. 3. Large areas of  $\text{PM}_{2.5}$  enhancement are found in northern and eastern China with  $\text{PM}_{2.5}$  concentrations of  $70\text{--}130 \mu\text{g}/\text{m}^3$  in most regions, and values above  $130 \mu\text{g}/\text{m}^3$  in the major industrialized areas. It is believed that rapid economic development and associated industrial activities in northern and eastern China are the causes of the severe  $\text{PM}_{2.5}$  pollution, especially in the North China Plain (Quan et al., 2011; Wang, Wei, Yang, Zhang, Zhang, Su, et al., 2014). There is a band of heavy  $\text{PM}_{2.5}$  pollution zone cross over north central Shanxi and Shaanxi, which are regions with large coal production and abundant coal-fired facilities. Another hotspot of high concentrations of  $\text{PM}_{2.5}$  lies in the Sichuan Basin, which is surrounded by mountains and experiences adverse pollution dispersion conditions. The emerging industrialized city clusters over Hubei and Hunan provinces are also places heavily affected by anthropogenic emissions, where a large area with  $\text{PM}_{2.5}$  concentration ( $90\text{--}120 \mu\text{g}/\text{m}^3$ ) was identified by this work. High  $\text{PM}_{2.5}$  concentrations are also found in less populated areas such as northwestern China, which are dominated by mineral dust from the Taklimakan Desert, the largest desert in China. The spatial distribution of  $\text{PM}_{2.5}$  is quite different from that of AOD, with northern China having higher values than eastern China, reflecting aerosols aloft in eastern China. This is supported by the CALIOP observations (see Fig. S2 in Supporting information).

An evaluation of the satellite-derived  $\text{PM}_{2.5}$  concentrations against surface measurements was conducted using the measurements collated

from published work. The locations of the monitoring sites used in this study are presented in Fig. 4a and the monitoring sites cover most of eastern China. We only use measurement data with sampling times of longer than one month and among all 68 sites, 46 sites have  $\text{PM}_{2.5}$  measurements for at least one year time (a whole year or one month in each season). The collected  $\text{PM}_{2.5}$  data are randomly distributed in time and space (see Table S1 in Supporting information), which are believed to be representative of the study time period and region. Before comparison with measurements data, the satellite derived  $\text{PM}_{2.5}$  concentrations are corrected using sampling correction factor at monthly-scale and then averaged to the corresponding measurement time, as defined in Eqs. ((2)–(3)). The comparison between the collated data and the mean value of the satellite-derived  $\text{PM}_{2.5}$  for the corresponding sampling period is shown in Fig. 4b. Significant agreement exists with  $r = 0.74$ , slope = 0.77 and intercept =  $11.21 \mu\text{g}/\text{m}^3$ .

We also compared satellite-derived  $\text{PM}_{2.5}$  concentrations with observations from the national  $\text{PM}_{2.5}$  monitoring network for Jan–May 2013 (We only conducted simulations for the first five months in 2013 because the GEOS-5 meteorological data at  $0.5^\circ \times 0.667^\circ$  resolution are not available afterward) as an additional support to our work, as presented in Fig. 5. Good correlation between the five-month-mean satellite-based  $\text{PM}_{2.5}$  concentration and the corresponding measurement data was found across China ( $r = 0.85$ , slope = 1.17, intercept =  $-19.71 \mu\text{g}/\text{m}^3$ ), although the satellite-derived data were biased a little high in regions above  $120 \mu\text{g}/\text{m}^3$  (Fig. 5b).

### 3.3. Errors

The errors in the long-term satellite-derived  $\text{PM}_{2.5}$  concentrations stem mainly from uncertainties in the AOD retrievals, accuracy of vertical aerosol profile in the model, and impact of incomplete sampling. After filtration, the AOD retrieval bias against ground-measurement AOD data lies within the larger bound of  $\pm 20\%$  or  $\pm 0.1$ , as regions with an expected bias exceeding that value are all excluded. The uncertainties in the modeled  $\text{PM}_{2.5}/\text{AOD}$  ratio are dominated by errors in the simulated relative vertical profile (van Donkelaar et al., 2006); however, despite this, it can be affected by emission inputs, meteorological conditions, and chemical processes in the model. The modeled relative

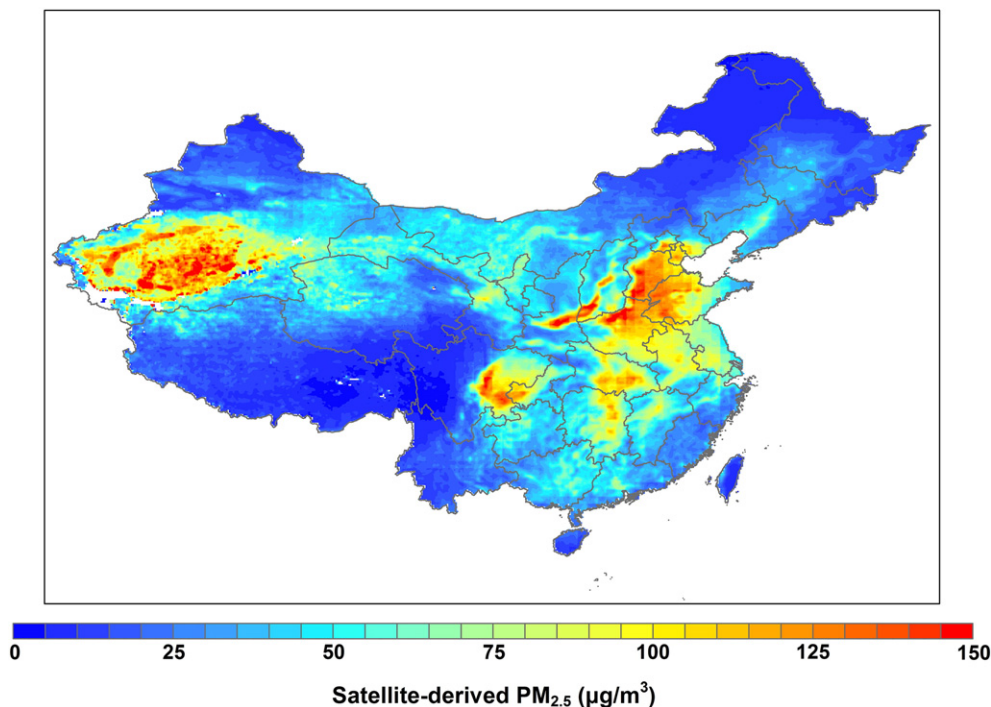
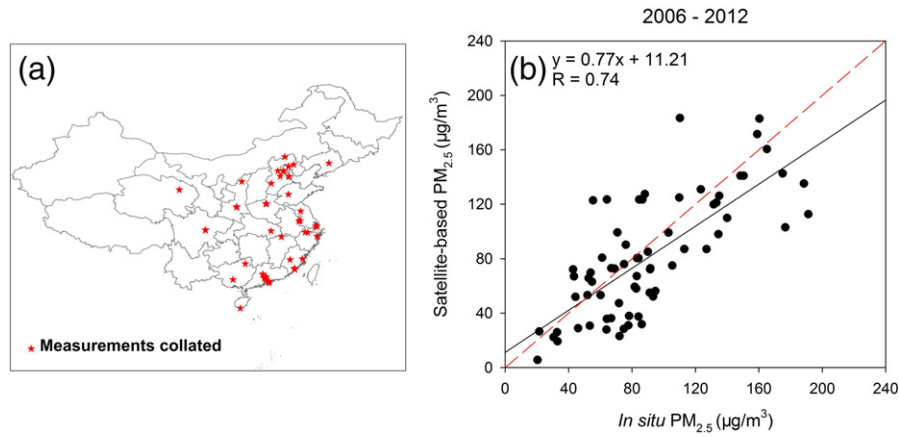


Fig. 3. Satellite-derived  $\text{PM}_{2.5}$  averaged over 2006–2012 in China. White space indicates less than 10 successful observations.



**Fig. 4.** Comparisons between satellite-derived  $PM_{2.5}$  and in situ data collected from publications. (a) Locations of ground measurement sites collated. (b) Comparison between measurements from publications and corresponding satellite-derived data for 2006–2012. The solid black line represents the best fit and the red dashed line shows the 1:1 line.

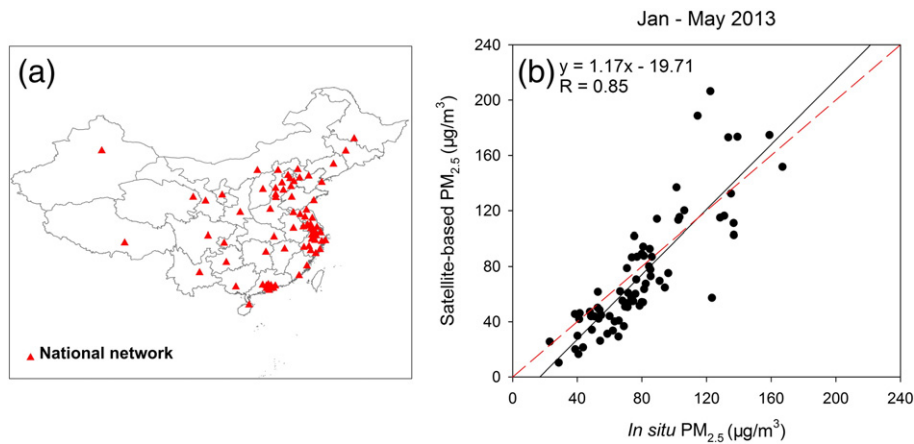
vertical profiles were evaluated and corrected using the observations from CALIOP (van Donkelaar et al., 2013; Winker et al., 2007). We used the standard deviation of the relative ratio between CALIOP and model simulation to represent errors in the relative profile. Incomplete sampling by the satellite can also introduce some bias compared with the continuous averaged value. The sampling bias is calculated as the difference between the continuous mean model  $PM_{2.5}$  concentrations and the coincidentally sampled simulated values. Then the total errors in the satellite-derived  $PM_{2.5}$  concentrations were combined in quadrature of three error sources above.

Fig. 6 shows the spatial distribution of the estimated errors from each source and the total errors in the satellite-derived  $PM_{2.5}$ . It can be seen that most regions have estimated errors within 25% of the satellite-derived value. In the most polluted region of the North China Plain, the bias can be reaching 30–35% (Fig. 6a). Profile errors are typically less than 20%; however, enhanced error is found in Sichuan Basin, possibly due to the large temporal variation in the relative profile ratio (Fig. 6b). Satellite AOD is usually missing in the presence of cloud, bright surfaces due to snow, or extremely high aerosol concentrations (van Donkelaar et al., 2011). These missing AOD values are heterogeneous among seasons, which might cause a systematic bias because  $PM_{2.5}$  concentrations have large seasonal variability in China. As can be seen from Fig. 6c, most regions have sampling bias within  $\pm 20\%$ : negative bias in northern China and positive bias in the south. This is because in northern China, there are more AOD values missing in winter due to bright surfaces caused by snow, low-level clouds and more

frequent haze days (the satellite algorithm may regard heavy haze as clouds), and  $PM_{2.5}$  concentrations are shown to peak in winter. In southern China, frequent rainfall in summer causes more missing values of AOD and  $PM_{2.5}$  concentrations in summer are the lowest of the entire year.

### 3.4. Population exposure to $PM_{2.5}$

Long-term exposures to outdoor ambient  $PM_{2.5}$  were estimated for China at a resolution of  $0.1^\circ \times 0.1^\circ$  using our satellite-derived  $PM_{2.5}$  concentrations for 2006–2012, in conjunction with the LandScan Global Population database (ORNL, 2010, Bright, Coleman, Rose, & Urban, 2011). Table 1 presents the national and regional levels of long-term  $PM_{2.5}$  exposure. The population-weighted mean  $PM_{2.5}$  concentration over China is  $71 \mu\text{g}/\text{m}^3$ , which is much higher than in North American and Europe (van Donkelaar et al., 2010). As can be seen, less than 1% of the Chinese population lives in conditions with concentrations of  $PM_{2.5}$  below the World Health Organization (WHO) Air Quality Guideline (AQG) of  $10 \mu\text{g}/\text{m}^3$  (WHO, 2005). China is now using the WHO Air Quality Interim Target-1 of  $35 \mu\text{g}/\text{m}^3$  as the level 2 annual  $PM_{2.5}$  standard, which is designated for residential, mixed commercial/residential, cultural, industrial and rural areas, according to CNAAQs. However, approximately 1.1 billion people (82% of total population) in China reside in places exceeding the CNAAQs level 2 annual standard, and there are more than 330 million people (25% of total) living in regions with  $PM_{2.5}$  levels higher than  $100 \mu\text{g}/\text{m}^3$ . Of the four



**Fig. 5.** Comparisons between satellite-derived  $PM_{2.5}$  and in situ data from national networks. (a) Locations of ground measurement sites from national networks. (b) Comparison between measurements from national ground-based measurements and corresponding satellite-derived data for Jan–May 2013. The solid black line represents the best fit and the red dashed line shows the 1:1 line.

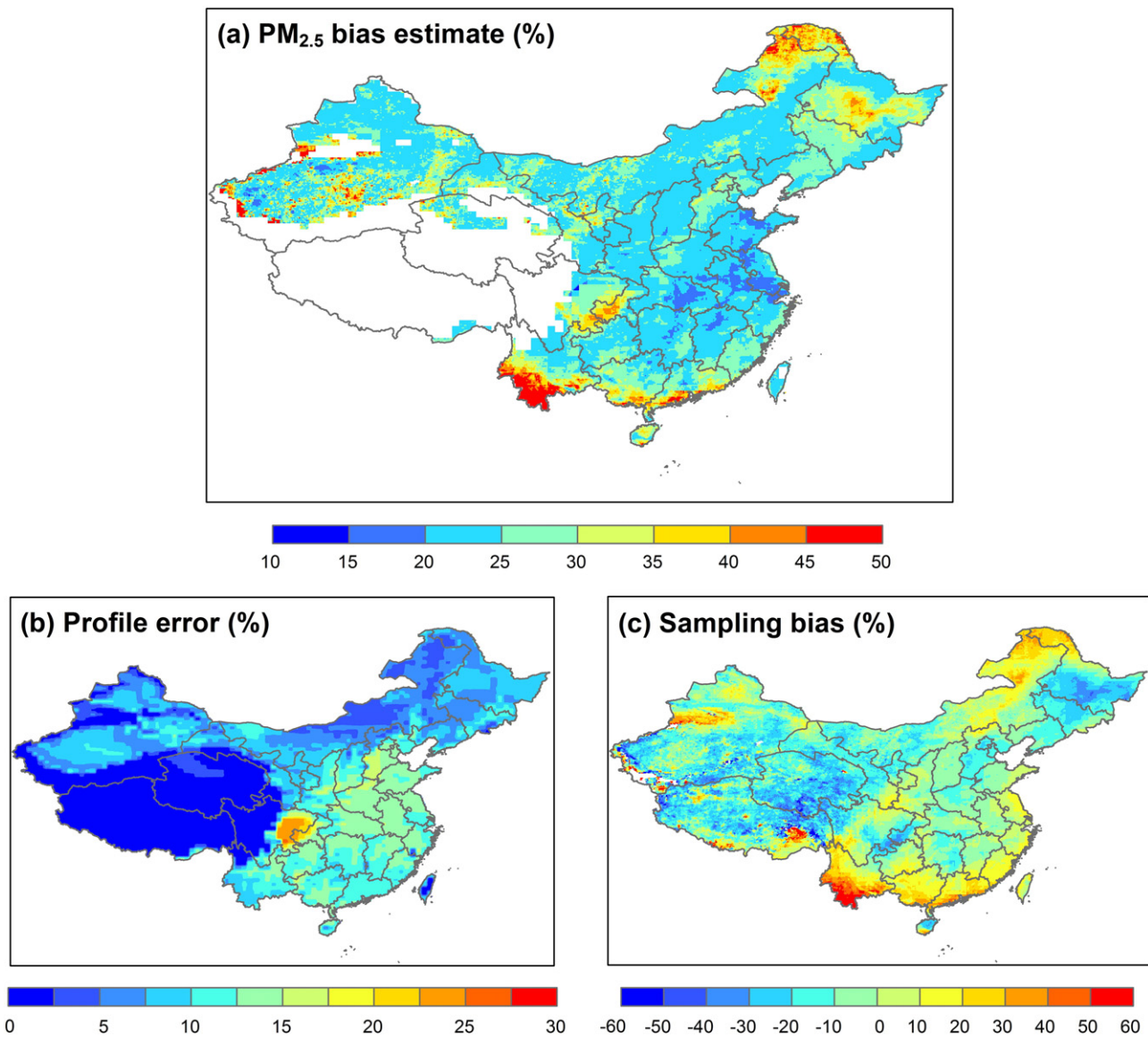


**Fig. 6.** Uncertainties in the satellite-derived PM<sub>2.5</sub> concentrations. (a) Estimate of the satellite-derived PM<sub>2.5</sub> bias. (b) Errors in the aerosol vertical profiles. (c) Percentage change of the coincidentally sampled simulated PM<sub>2.5</sub> concentrations relative to the continuous mean model value.

selected regions, northern China, which covers the political and economic center and accommodates 23% of the national population, has the highest PM<sub>2.5</sub> level with a population-weighted mean reaching 104  $\mu\text{g}/\text{m}^3$  which exceeds the national standard by a factor of 3. Only 3% people of this region are lived in the areas where can meet level 2 annual standard. Conversely, southern China has much lower PM<sub>2.5</sub> concentrations with a population-weighted mean value of 44  $\mu\text{g}/\text{m}^3$ , which is 26% higher than the national standard.

#### 4. Discussion

Epidemiological studies and health impact assessments largely rely on measurements of the ambient ground-level fine PM (Cao, Xu, Xu, Chen, & Kan, 2012). However, ground-based monitoring networks are very limited, especially in China, which has the largest population and highest air pollution levels in the world. Although China implemented a national monitoring network in 2013, the monitoring sites are sparse

**Table 1**  
Regional population-weighted PM<sub>2.5</sub> concentration and population in excess of certain PM<sub>2.5</sub> levels calculated from this work for 2006–2012 and the previous estimates of van Donkelaar et al. (2010) for 2001–2006 (referred to as Previous).

| Region         | Population-weighted mean ( $\mu\text{g}/\text{m}^3$ ) |          | Population (million) |                              |           |                              |           |                               |           |
|----------------|---|----------|----------------------|------------------------------|-----------|------------------------------|-----------|-------------------------------|-----------|
|                | This work   | Previous | Total                | >10 $\mu\text{g}/\text{m}^3$ |           | >35 $\mu\text{g}/\text{m}^3$ |           | >100 $\mu\text{g}/\text{m}^3$ |           |
|                |   |          | This work            | Previous                     | This work | Previous                     | This work | Previous                      | This work |
| Northern China | 103.8   | 72.5     | 303                  | 303                          | 303       | 293                          | 271       | 200                           | 6         |
| Eastern China  | 78.2  | 64.7     | 359                  | 359                          | 359       | 342                          | 337       | 62                            | 3         |
| Southern China | 44.0  | 40.2     | 153                  | 153                          | 151       | 100                          | 97        | 0                             | 0         |
| Sichuan Basin  | 87.1  | 64.6     | 137                  | 137                          | 135       | 130                          | 116       | 48                            | 15        |
| China          | 71.4  | 53.0     | 1345                 | 1334                         | 1293      | 1100                         | 935       | 331                           | 24        |

and representative of only a small part of the entire country. Furthermore, there are still no regular monitoring data for levels of PM<sub>2.5</sub> exposure in the past. Satellite remote sensing provides spatially and temporally continuous information on aerosols in the atmosphere, which can supplement ground-based measurements by filling gaps in the measurement dataset (Crouse et al., 2012; Evans et al., 2013).

In this study, we generated a long-term (2006–2012) mean spatial distribution of PM<sub>2.5</sub> concentrations over China using MODIS and MISR satellite observations and the nested-grid GEOS-Chem chemical transport model. We compared our results with the satellite-based 2001–2006 global PM<sub>2.5</sub> concentrations in van Donkelaar et al. (2010), which was used in the Global Burden of Disease Study 2010 together with the simulations from global TM5 model to describe the health risks caused by fine particles (Brauer et al., 2011). The PM<sub>2.5</sub> concentrations over China derived in this study are substantially higher than those reported in van Donkelaar et al. (2010), especially in heavily polluted regions. According to van Donkelaar et al. (2010), only 24 million people in China live in areas where PM<sub>2.5</sub> concentrations exceed 100 µg/m<sup>3</sup>, which is a much smaller number than that proposed in this work (Table 1).

The difference between these two studies likely resulted from both in the different periods studied and from the improvements implemented in our method. During 2006–2012, the average emissions of major PM<sub>2.5</sub> precursors in China are estimated to be higher than emissions during 2001–2006 (Fig. S3), while SO<sub>2</sub> emissions in China have been decreased after 2006 (Lu, Zhang, & Streets, 2011). Additionally, we replaced the global model with a nested-grid model, which has a finer resolution of 0.5° × 0.667° and can more accurately capture the variations of the conversion factors between AOD and PM<sub>2.5</sub> on a local scale. We also utilized observations from CALIOP to correct the vertical profiles in the model simulation, which is the most important factor affecting the relationship between AOD and PM<sub>2.5</sub>. All data including emission inventories and satellite retrievals were updated to 2006–2012. All of which could contribute to the differences between two estimates. Therefore, the mortality and morbidity caused by ambient PM<sub>2.5</sub> concentrations could be even higher than found in the Global Burden of Disease Study 2010.

We also compared our results with Ma et al. (2014) which also focused on satellite-based PM<sub>2.5</sub> estimates in China but using GWR model. The two datasets have very similar spatial structures, while our work is higher than that in Ma et al. (2014), especially in the heavily polluted regions, with a mean concentration over the North China Plain of 110–150 µg/m<sup>3</sup> compared to 85–95 µg/m<sup>3</sup>. This difference may arise because the current GWR model tends to underestimate PM<sub>2.5</sub> concentration in heavily polluted regions (Hoff & Christopher, 2009; Liu, Sarnat, Kilaru, Jacob, & Koutrakis, 2005) and the AOD values are missing during severe haze days.

Our work is an update and improvement of the satellite-derived PM<sub>2.5</sub> concentrations in China based on previous work (van Donkelaar et al., 2010). However, many directions still need to be taken to improve the satellite-derived PM<sub>2.5</sub> concentrations. In the current method of combining MODIS and MISR AOD data, although we used the ground measurements as a constraint to screen the satellite retrieval before merging two products, the biases may not be entirely eliminated due to the sparse spatial distribution of the ground measurements. In the current operational satellite AOD product, pixels with 0.47 mm reflectance > 0.4 are considered cloudy and retrieved AOD > 5.0 is removed (Remer, Tanré, Kaufman, Levy, & Mattoo, 2006). These strict criteria improved the data quality but might miss AOD while during heavy haze days because they were mistaken for cloud or exceed 5.0 (van Donkelaar et al., 2011). Improvements in the satellite retrieval algorithm could help to yield better satellite coverage in conditions of high pollution level and reduce sampling biases. The enhanced formation of sulfate and nitrate during haze pollutions by heterogeneous chemistry (Wang, Yao, Wang, Liu, Ji, Tang, et al., 2014; Wang et al., 2012) and the interaction between aerosol and planetary boundary

layers (Ding et al., 2013) are not included in the GEOS-chem model, which may lead to the underestimation of PM<sub>2.5</sub> concentrations and bias in aerosol profiles during heavily polluted days (Zheng et al., 2015). Future developments in the model capabilities for aerosols could improve the estimation of the conversion factors. Besides, the monitoring sites used in this study are concentrated in urban regions and limited over rural areas, which makes it less confident in clean regions. However, this situation might be improved as more ground monitoring data will be established in the Chinese national and regional air quality monitoring network, including rural sites, which could provide additional inputs to develop and evaluate the satellite-derived database in the future.

## 5. Conclusion

Our work is an improvement and update of the satellite-derived PM<sub>2.5</sub> concentrations in China based on previous work. We replaced the global model with a nested-grid model, which has a finer resolution of 0.5° × 0.667° and provides the conversion factors between AOD and PM<sub>2.5</sub> on a local scale. We also utilized observations from CALIOP to correct the vertical profiles in the model simulation. All data including emission inventories and satellite retrievals were updated to 2006–2012. We found significant spatial agreement between the corresponding satellite-derived and ground-based PM<sub>2.5</sub> observations using both the national network dataset ( $r = 0.85$ , slope = 1.17, intercept = -19.71 µg/m<sup>3</sup>) and PM<sub>2.5</sub> data collated from literatures ( $r = 0.74$ , slope = 0.77, intercept = 11.21 µg/m<sup>3</sup>).

Our results suggest that the population-weighted geometric mean of PM<sub>2.5</sub> concentration is 71 µg/m<sup>3</sup> over China and that less than 1% of the Chinese population resides in regions with PM<sub>2.5</sub> concentrations under the WHO AQG limit of 10 µg/m<sup>3</sup>. Moreover, 82% of the population lives in locations where the PM<sub>2.5</sub> concentrations exceed the level 2 annual PM<sub>2.5</sub> standard. Such high levels of PM<sub>2.5</sub> exposure will cause an increase in the risk of air-pollution-related health impacts. Population exposure estimated from this dataset could facilitate studies into the long-term exposure to PM<sub>2.5</sub> in China.

## Acknowledgments

This study was supported by the National Science Foundation of China (41222036, 41275026, 71322304, and 41175127). Q. Zhang and K. B. He are supported by the Collaborative Innovation Center for Regional Environmental Quality. The work at Dalhousie was supported by the Natural Sciences and Engineering Research Council of Canada (5265-417449-12). We thank the two anonymous reviewers for their constructive comments.

## Appendix A. Supplementary data

Supplementary data to this article can be found online at <http://dx.doi.org/10.1016/j.rse.2015.05.016>.

## References

- Beckerman, B. S., Jerrett, M., Serre, M., Martin, R. V., Lee, S. -J., van Donkelaar, A., et al. (2013). A hybrid approach to estimating national scale spatiotemporal variability of PM<sub>2.5</sub> in the contiguous United States. *Environmental Science and Technology*, 47(13), 7233–7241.
- Brauer, M., Amann, M., Burnett, R. T., Cohen, A., Dentener, F., Ezzati, M., et al. (2011). Exposure assessment for estimation of the global burden of disease attributable to outdoor air pollution. *Environmental Science and Technology*, 46(2), 652–660.
- Bright, E. A., Coleman, P. R., Rose, A. N., & Urban, M. L. (2011). *LandScan 2010*. Oak Ridge, TN: Oak Ridge National Laboratory.
- Cao, J., Xu, H., Xu, Q., Chen, B., & Kan, H. (2012). Fine particulate matter constituents and cardiopulmonary mortality in a heavily polluted Chinese city. *Environmental Health Perspectives*, 120(3), 373–378.
- Che, H., Yang, Z., Zhang, X., Zhu, C., Ma, Q., Zhou, H., et al. (2009). Study on the aerosol optical properties and their relationship with aerosol chemical compositions over three regional background stations in China. *Atmospheric Environment*, 43(5), 1093–1099.

- Che, H., Zhang, X., Chen, H., Damiri, B., Goloub, P., Li, Z., et al. (2009). Instrument calibration and aerosol optical depth validation of the China Aerosol Remote Sensing Network. *Journal of Geophysical Research*, 114(D3), D03206.
- Chen, W.-T., Kahn, R. A., Nelson, D., Yau, K., & Seinfeld, J. H. (2008). Sensitivity of multiangle imaging to the optical and microphysical properties of biomass burning aerosols. *Journal of Geophysical Research*, 113(D10), D10203.
- Chu, D. A., Kaufman, Y. J., Zibordi, G., Chern, J. D., Mao, J., Li, C. C., et al. (2003). Global monitoring of air pollution over land from the Earth Observing System-Terra Moderate Resolution Imaging Spectroradiometer (MODIS). *Journal of Geophysical Research*, 108(D21).
- Crouse, D. L., Peters, P. A., van Donkelaar, A., Goldberg, M. S., Villeneuve, P. J., Brion, O., et al. (2012). Risk of nonaccidental and cardiovascular mortality in relation to long-term exposure to low concentrations of fine particulate matter: A Canadian national-level cohort study. *Environmental Health Perspectives*, 120(5), 708–714.
- Diner, D. J., Beckert, J. C., Reilly, T. H., Bruegge, C. J., Conel, J. E., Kahn, R. A., et al. (1998). Multi-angle Imaging Spectroradiometer (MISR) – Instrument description and experiment overview. *IEEE Transactions on Geoscience and Remote Sensing*, 36(4), 1072–1087.
- Ding, A. J., Fu, C. B., Yang, X. Q., Sun, J. N., Petäjä, T., Kerminen, V. M., et al. (2013). Intense atmospheric pollution modifies weather: A case of mixed biomass burning with fossil fuel combustion pollution in eastern China. *Atmospheric Chemistry and Physics*, 13(20), 10545–10554.
- Dockery, D. W., Pope, C. A., Xu, X. P., Spengler, J. D., Ware, J. H., Fay, M. E., et al. (1993). An association between air-pollution and mortality in 6 United-States cities. *The New England Journal of Medicine*, 329(24), 1753–1759.
- Engel-Cox, J. A., Hoff, R. M., & Haymet, A. D. J. (2004). Recommendations on the use of satellite remote-sensing data for urban air quality. *Journal of the Air and Waste Management Association*, 54(11), 1360–1371.
- Evans, J., van Donkelaar, A., Martin, R. V., Burnett, R., Rainham, D. G., Birkett, N. J., et al. (2013). Estimates of global mortality attributable to particulate air pollution using satellite imagery. *Environmental Research*, 120, 33–42.
- Ford, B., & Heald, C. L. (2012). An A-train and model perspective on the vertical distribution of aerosols and CO in the Northern Hemisphere. *Journal of Geophysical Research*, 117(D6), D06211.
- Hoff, R. M., & Christopher, S. A. (2009). Remote sensing of particulate pollution from space: Have we reached the promised land? *Journal of the Air and Waste Management Association*, 59(6), 645–675.
- Holben, B. N., Eck, T. F., Slutsker, I., Tanre, D., Buis, J. P., Setzer, A., et al. (1998). AERONET – A federated instrument network and data archive for aerosol characterization. *Remote Sensing of Environment*, 66(1), 1–16.
- Hu, X., Waller, L. A., Al-Hamdan, M. Z., Crosson, W. L., Estes, M. G., Jr., Estes, S. M., et al. (2013). Estimating ground-level PM<sub>2.5</sub> concentrations in the southeastern US using geographically weighted regression. *Environmental Research*, 121, 1–10.
- Hu, X., Waller, L. A., Lyapustin, A., Wang, Y., Al-Hamdan, M. Z., Crosson, W. L., et al. (2014). Estimating ground-level PM<sub>2.5</sub> concentrations in the Southeastern United States using MAIAC AOD retrievals and a two-stage model. *Remote Sensing of Environment*, 140, 220–232.
- Kahn, R. A., Banerjee, P., McDonald, D., & Diner, D. J. (1998). Sensitivity of multiangle imaging to aerosol optical depth and to pure-particle size distribution and composition over ocean. *Journal of Geophysical Research*, 103(D24), 32195–32213.
- Kahn, R. A., Gaitley, B. J., Garay, M. J., Diner, D. J., Eck, T. F., Smirnov, A., et al. (2010). Multiangle Imaging Spectroradiometer global aerosol product assessment by comparison with the Aerosol Robotic Network. *Journal of Geophysical Research*, 115(D23), D23209.
- Kahn, R. A., Garay, M. J., Nelson, D. L., Yau, K. K., Bull, M. A., Gaitley, B. J., et al. (2007). Satellite-derived aerosol optical depth over dark water from MISR and MODIS: Comparisons with AERONET and implications for climatological studies. *Journal of Geophysical Research*, 112(D18), D18205.
- Kahn, R. A., Li, W. H., Moroney, C., Diner, D. J., Martonchik, J. V., & Fishbein, E. (2007). Aerosol source plume physical characteristics from space-based multiangle imaging. *Journal of Geophysical Research*, 112(D11).
- Kloog, I., Nordio, F., Coull, B. A., & Schwartz, J. (2012). Incorporating local land use regression and satellite aerosol optical depth in a hybrid model of spatiotemporal PM<sub>2.5</sub> exposures in the mid-Atlantic states. *Environmental Science and Technology*, 46(21), 11913–11921.
- Lee, H. J., Liu, Y., Coull, B. A., Schwartz, J., & Koutrakis, P. (2011). A novel calibration approach of MODIS AOD data to predict PM<sub>2.5</sub> concentrations. *Atmospheric Chemistry and Physics*, 11(15), 7991–8002.
- Levy, R. C., Remer, L. A., Mattoo, S., Vermote, E. F., & Kaufman, Y. J. (2007). Second-generation operational algorithm: Retrieval of aerosol properties over land from inversion of Moderate Resolution Imaging Spectroradiometer spectral reflectance. *Journal of Geophysical Research*, 112(D13).
- Lin, J., van Donkelaar, A., Xin, J., Che, H., & Wang, Y. (2014). Clear-sky aerosol optical depth over East China estimated from visibility measurements and chemical transport modeling. *Atmospheric Environment*, 95, 258–267.
- Liu, Y., Park, R. J., Jacob, D. J., Li, Q. B., Kilaru, V., & Sarnat, J. A. (2004). Mapping annual mean ground-level PM<sub>2.5</sub> concentrations using Multiangle Imaging Spectroradiometer aerosol optical thickness over the contiguous United States. *Journal of Geophysical Research*, 109(D22).
- Liu, Y., Sarnat, J. A., Kilaru, V., Jacob, D. J., & Koutrakis, P. (2005). Estimating ground-level PM<sub>2.5</sub> in the Eastern United States using satellite remote sensing. *Environmental Science & Technology*, 39(9), 3269–3278.
- Lu, Z., Zhang, Q., & Streets, D. G. (2011). Sulfur dioxide and primary carbonaceous aerosol emissions in China and India, 1996–2010. *Atmospheric Chemistry and Physics*, 11(18), 9839–9864.
- Ma, Z., Hu, X., Huang, L., Bi, J., & Liu, Y. (2014). Estimating ground-level PM<sub>2.5</sub> in China using satellite remote sensing. *Environmental Science and Technology*, 48(13), 7436–7444.
- Martin, R. V. (2008). Satellite remote sensing of surface air quality. *Atmospheric Environment*, 42(34), 7823–7843.
- McDonnell, W. F., Nishino-Ishikawa, N., Petersen, F. F., Chen, L. H., & Abbey, D. E. (2000). Relationships of mortality with the fine and coarse fractions of long-term ambient PM<sub>10</sub> concentrations in nonsmokers. *Journal of Exposure Analysis and Environmental Epidemiology*, 10(5), 427–436.
- Pope, C. A., Burnett, R. T., Thun, M. J., Calle, E. E., Krewski, D., Ito, K., et al. (2002). Lung cancer, cardiopulmonary mortality, and long-term exposure to fine particulate air pollution. *JAMA*, 287(9), 1132–1141.
- Quan, J., Zhang, Q., He, H., Liu, J., Huang, M., & Jin, H. (2011). Analysis of the formation of fog and haze in North China Plain (NCP). *Atmospheric Chemistry and Physics*, 11(15), 8205–8214.
- Remer, L. A., Kaufman, Y. J., Tanre, D., Mattoo, S., Chu, D. A., Martins, J. V., et al. (2005). The MODIS aerosol algorithm, products, and validation. *Journal of the Atmospheric Sciences*, 62(4), 947–973.
- Remer, L. A., Tanre, D., Kaufman, Y. J., Levy, R. C., & Mattoo, S. (2006). *Algorithm for remote sensing of tropospheric aerosol from MODIS: Collection 005*. Algorithm Theoretical Basis Document.
- Schaaf, C. B., Gao, F., Strahler, A. H., Lucht, W., Li, X. W., Tsang, T., et al. (2002). First operational BRDF, albedo nadir reflectance products from MODIS. *Remote Sensing of Environment*, 83(1–2), 135–148.
- Sun, J., Zhang, M., & Liu, T. (2001). Spatial and temporal characteristics of dust storms in China and its surrounding regions, 1960–1999: Relations to source area and climate. *Journal of Geophysical Research*, 106(D10), 10325–10333.
- Toth, T. D., Zhang, J., Campbell, J. R., Hyer, E. J., Reid, J. S., Shi, Y., et al. (2014). Impact of data quality and surface-to-column representativeness on the PM<sub>2.5</sub> / satellite AOD relationship for the contiguous United States. *Atmospheric Chemistry and Physics*, 14(12), 6049–6062.
- van Donkelaar, A., Martin, R. V., Brauer, M., Kahn, R., Levy, R., Verduzco, C., et al. (2010). Global estimates of ambient fine particulate matter concentrations from satellite-based aerosol optical depth: Development and application. *Environmental Health Perspectives*, 118(6), 847–855.
- van Donkelaar, A., Martin, R. V., Levy, R. C., da Silva, A. M., Krzyzanowski, M., Chubarova, N. E., et al. (2011). Satellite-based estimates of ground-level fine particulate matter during extreme events: A case study of the Moscow fires in 2010. *Atmospheric Environment*, 45(34), 6225–6232.
- van Donkelaar, A., Martin, R. V., & Park, R. J. (2006). Estimating ground-level PM<sub>2.5</sub> using aerosol optical depth determined from satellite remote sensing. *Journal of Geophysical Research*, 111(D21), D21201.
- van Donkelaar, A., Martin, R. V., Spurr, R. J. D., Drury, E., Remer, L. A., Levy, R. C., et al. (2013). Optimal estimation for global ground-level fine particulate matter concentrations. *Journal of Geophysical Research*, 118(11), 5621–5636.
- Wang, J., & Christopher, S. A. (2003). Intercomparison between satellite-derived aerosol optical thickness and PM<sub>2.5</sub> mass: Implications for air quality studies. *Geophysical Research Letters*, 30(21).
- Wang, X., Wang, W., Yang, L., Gao, X., Nie, W., Yu, Y., et al. (2012). The secondary formation of inorganic aerosols in the droplet mode through heterogeneous aqueous reactions under haze conditions. *Atmospheric Environment*, 63, 68–76.
- Wang, L. T., Wei, Z., Yang, J., Zhang, Y., Zhang, F. F., Su, J., et al. (2014). The 2013 severe haze over southern Hebei, China: Model evaluation, source apportionment, and policy implications. *Atmospheric Chemistry and Physics*, 14(6), 3151–3173.
- Wang, Y., Yao, L., Wang, L., Liu, Z., Ji, D., Tang, G., et al. (2014). Mechanism for the formation of the January 2013 heavy haze pollution episode over central and eastern China. *Science China Earth Sciences*, 57(1), 14–25.
- WHO (World Health Organization) (2005). *Air quality guidelines global update 2005*. Copenhagen, Denmark: WHO/Europe.
- Winker, D. M., Hunt, W. H., & McGill, M. J. (2007). Initial performance assessment of CALIOP. *Geophysical Research Letters*, 34(19), L19803.
- Yang, F., Tan, J., Zhao, Q., Du, Z., He, K., Ma, Y., et al. (2011). Characteristics of PM<sub>2.5</sub> speciation in representative megacities and across China. *Atmospheric Chemistry and Physics*, 11(11), 5207–5219.
- Zhang, H., Hoff, R. M., & Engel-Cox, J. A. (2009). The relation between moderate resolution imaging spectroradiometer (MODIS) aerosol optical depth and PM<sub>2.5</sub> over the United States: A geographical comparison by US Environmental Protection Agency regions. *Journal of the Air and Waste Management Association*, 59(11), 1358–1369.
- Zhang, Q., Streets, D. G., Carmichael, G. R., He, K. B., Huo, H., Kannari, A., et al. (2009). Asian emissions in 2006 for the NASA INTEX-B mission. *Atmospheric Chemistry and Physics*, 9(14), 5131–5153.
- Zheng, B., Zhang, Q., Zhang, Y., He, K. B., Wang, K., Zheng, G. J., et al. (2015). Heterogeneous chemistry: A mechanism missing in current models to explain secondary inorganic aerosol formation during the January 2013 haze episode in North China. *Atmospheric Chemistry and Physics*, 15(4), 2031–2049.